

WIND TUNNEL TESTS FOR GUST LOAD INVESTIGATION IN TRANSONIC FLOWS – PART 1 : DEVELOPMENT OF AN INNOVATIVE TEST RIG

A. Lepage¹, N. Paletta^{2*}, S. Russo³, S. Ricci⁴, E. Rantet⁵, A. Barnique⁶

¹ ONERA, Université Paris Saclay
29 avenue de la Division Leclerc 92320 Chatillon - France

² Airbus Defence and Space - Germany
* formerly Coordinator of the GUDGET project at IBK Innovation (Germany)

³ Dream Innovation Srl
Via F. Parri, 1, 81030, Sant'Arpino (CE) - Italy

⁴ Politecnico di Milano - Department of Aerospace Science and Technology
via La Masa 34, 20156 Milano - Italy

⁵ Aviation Design
ZA du Chenet, 5 rue des acacias, 91490 Milly-La-Forêt - France

⁶ Cedrat Technologies
59 Chemin du Vieux Chêne 38246 Meylan - France

Keywords: Wind Tunnel, Gust Load, Test Rig, Transonic Flows

Abstract: The development of load predictions capabilities and load control strategies is a key axis for enhancing the design process of the next aircraft generation, with the aim of significantly reducing fuel consumption levels. Within the Clean Sky 2 AIRFRAME ITD framework, a specific objective is dedicated to addressing the gust load case, which is crucial for strength design and fatigue loading source for transport type aircraft particularly in the certification process.

Building on the accomplishments of the Clean Sky SFWA-ITD project, a new experimental research program has been established, centred around Wind Tunnel Tests (WTT) conducted at the transonic ONERA S3Ch facility. The primary goals of this program were to deepen our understanding of gust effects, particularly in the non-linear domain, and to advance the maturity of load control approaches.

The initial phase of these studies has been conducted within the framework of a project called GUDGET, aimed at developing an innovative test rig for investigating gust loads, particularly challenging in the transonic regime. Based on pre-design solutions provided by ONERA, new gust generation devices have been analysed, designed and manufactured in order to deliver deterministic vertical and harmonic gusts with larger amplitude and in a wide frequency range.

Two main concepts consisting in a tandem of airfoils installed horizontally right upstream of the test section were studied, based on either dynamically moving airfoils or fixed vanes equipped with pulsed blowing slots.

To investigate the effects of gusts on the aerodynamic and aeroelastic behaviour of a model, the test rig also included a wall-mounted half-wing model. This model was heavily instrumented and equipped with a suitable aileron located close to the wingtip, which was remotely actuated using a high-frequency actuation system to demonstrate real-time active gust load alleviation.

Finally, the results of a first WTT campaign, carried out to qualify the unsteady flow induced by the various gust generation capabilities, are presented. The outcomes of a second WTT dedicated to analysing gust effects on the model aeroelastic behaviour for different structural and aerodynamic conditions, are presented in a companion paper [12].

1 INTRODUCTION

ACARE (Advisory Council for Aeronautics Research in Europe) [1], through its Strategic Research and Innovation Agenda, imposes stringent demands on the aviation industry for the development of significantly more environmentally sustainable aircraft. These demands necessitate substantial reductions in fuel consumption, emissions, and perceived noise levels, with the overarching goal of environmental footprint reduction and energy savings.

The mission of Joint Technology Initiative Clean Sky 2 European research program is to develop breakthrough technologies to significantly increase the environmental performances of airplanes and air transport according to the ACARE Flightpath 2050. Within the framework of AIRFRAME-ITD [2], one of the key research axes is on the load control topic to contribute to both the reduction of the global aircraft weight and the improvement of passengers comfort and security.

One task associated to the demonstration plan strategy is dedicated to the analysis of wind tunnel gust load case, which is one of the most critical case for strength design and fatigue loading source for transport type aircraft. Within the previous program Clean Sky SFWA-ITD, Wind Tunnel test campaigns provided first database and results in transonic flow conditions. The main objective in Clean Sky 2 AIRFRAME ITD is to go further, to gain knowledge on gust effects (especially in the non-linear domain when encountering a gust) and to increase the maturity of load control approaches. Meanwhile, the acquisition of a relevant database is essential to assess the numerical capabilities for loads prediction to improve the design process of the next aircraft generation. So far, the load prediction methodologies are usually based on conservative approaches resulting in aircraft structures with unnecessary weight. Any improvement in this field has a strong impact on the margin sizing and leads to the design of lighter aircrafts. In addition, the development of innovative set-ups allows to assess and to de-risk the potential of advanced active load alleviation strategies in a research environment.

To reach these objectives, ONERA defined a new experimental research program based on Wind Tunnel Test (WTT) campaigns in the ONERA S3Ch facility. In this context, ONERA launched a call for proposal for the design and manufacturing of an innovative test rig. After the entire process, the GUDGET proposal was selected with IBK-Innovation GmbH, Dream Innovation srl, Politecnico di Milano, Aviation Design and Cedrat Technologies SA as consortium partners.

For the experimental investigation, the test rig is composed of two main items as illustrated in the Figure 1:

- an innovative gust generator to produce larger aerodynamic deflections than those obtained from an already existing device. The top objective is to be able to investigate non linearities induced by gust,
- a wall-mounted 3D wing model in order to analyse a more realistic configuration than the ones investigated within Clean Sky SFWA-ITD and restricted to 2D-airfoil configuration.

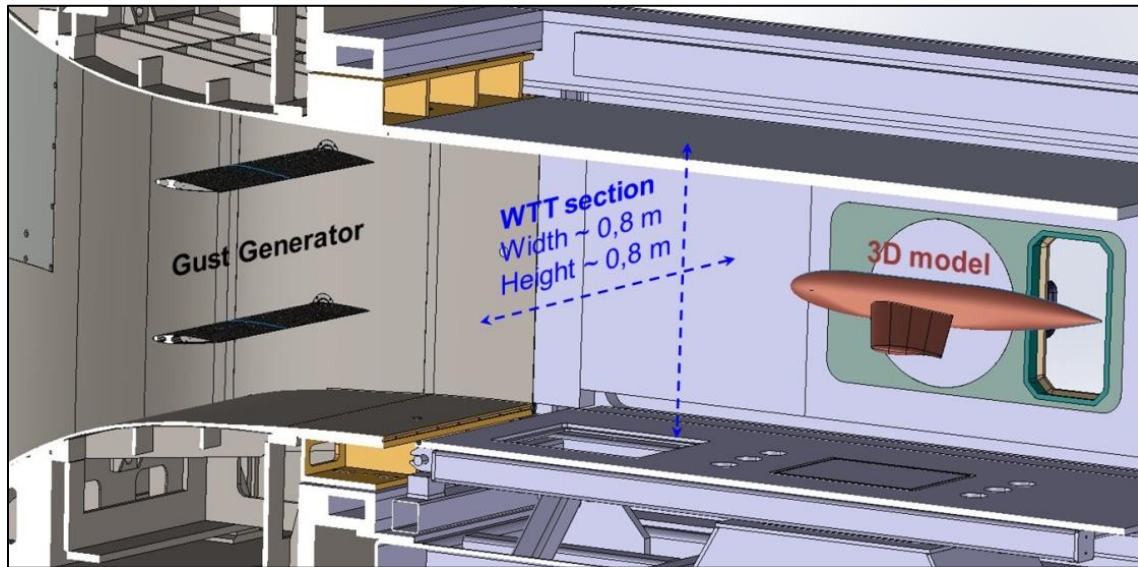


Figure 1 : Overview of the innovative test rig for the experimental gust load investigation

The two next sections present general considerations on the gust generation capabilities in a wind tunnel environment. A brief state of the art and a simplified modelling approach are introduced to document the key functioning parameters of gust generation, keeping the architecture of the previous ONERA apparatus [6] as the baseline (.i.e two oscillating airfoils). Then the results of parametric studies and CFD simulations, performed by the GUDGET partners, are presented to derive optimized configurations or innovative concepts of gust generator. The experimental test setups for gust generation designed and manufactured by the GUDGET consortium were assessed during a first WTT campaign and a short overview of the main outcomes is presented. Finally, the WTT model, which allows the investigation of gust effects on the aerodynamic and aeroelastic behaviour and the real time demonstration of active gust load alleviation functions, is described. The main concepts, design and manufacturing outcomes are briefly illustrated while the WTT campaign results are presented in a companion paper [12].

2 GUST LOAD INVESTIGATION IN WIND TUNNEL ENVIRONMENT

2.1 Existing Gust Generation Apparatus and project objectives

In the field of WTT for gust load investigation or alleviation, the gust generation apparatus is an essential device. Hence, many universities or research institutes have designed their own capability to generate gust fields, such as rotating slotted cylinder type, oscillating vane, cascade oscillating airfoil ... The reference [3] presents a summary of the different gust generators that have been in operation during the past 50 years (up to 2017) and emphasising the interest for the topic, as illustrated in Table 1.

Research Institute/University	Year	Top speed	Wind tunnel cross section
NASA (USA) (Reed 1981)	1966	Mach 1.2	Square $4.9 \times 4.9 \text{ m}^2$
MIT (USA) (Ham, Bauer <i>et al.</i> 1974)	1974	37 m/s	Elliptical $2.13 \times 3.32 \text{ m}^2$
Duke University (USA) (Tang, Cizmas <i>et al.</i> 1996)	1996	25 m/s	Rectangular $0.7 \times 0.53 \text{ m}^2$
Virginia Tech (USA) (Grissom and Devenport 2004)	2004	15 m/s	Square $2.15 \times 2.15 \text{ m}^2$
TSAGI (Russia) (Kuzmina, Ishmuratov <i>et al.</i> 2005)	2005	30 m/s	Elliptical $4.0 \times 2.33 \text{ m}^2$
TSAGI (Russia) (Kuzmina, Ishmuratov <i>et al.</i> 2005)	2005	120 m/s	Circular 7 m diameter
University of Maryland (USA) (Koushik and Schmitz 2007)	2008	N/A	N/A
Politecnico di Milano (Italy) (Ricci and Scotti 2008)	2008	30 m/s	Rectangular $1.0 \times 1.5 \text{ m}^2$
University of Colorado (USA) (Roadman and Mohseni 2009)	2009	20 m/s	Square $0.34 \times 0.34 \text{ m}^2$
DLR (Germany) (Neumann and Mai 2013)	2010	Mach 0.75	Square $1.0 \times 1.0 \text{ m}^2$
ONERA (France) (Lepage, Amosse <i>et al.</i> 2015)	2011	Mach 0.73	Rectangular $0.76 \times 0.8 \text{ m}^2$
Beihang University (China) (Wu, Chen <i>et al.</i> 2013)	2012	24 m/s	Square $3 \times 3 \text{ m}^2$
Cal Poly Pomona (USA) (YouTube video)	2013	61 m/s	Rectangular $1.0 \times 0.71 \text{ m}^2$
Cranfield University (England) (Saddington, Finnis <i>et al.</i> 2014)	2015	14.5 m/s	Elliptical $1.52 \times 1.14 \text{ m}^2$
ARA (England) (Allen and Quinn 2015)	2015	Mach 0.85	Rectangular $2.74 \times 2.44 \text{ m}^2$
Politecnico di Milano (Italy) (Ricci, Adden <i>et al.</i> 2015)	2016	55 m/s	Rectangular $4.0 \times 3.84 \text{ m}^2$
Mitsui engineering (Japan) (San technologies website)	N/A	20 m/s	N/A
JAXA (Japan) (Kenichi, Shunsuke <i>et al.</i> 2015)	N/A	Transonic	N/A

Table 1 - Summary of existing gust generator installations around the world from Lancelot et Al. 2017 [3]

However, there are few works conducted on the experimental investigation of gust in the transonic regime. Studies have been mostly performed in the low speed regime based on various mechanisms for creating an oscillating flow often based on the most common oscillating airfoils concept (Politecnico di Milano, Cranfield, University, Beihang University, Tsagi, Delft University ...).

In the transonic speed range, very few wind tunnel experiments can be identified: concepts based on oscillating vanes (NASA) or using a single (DLR) or two pitching airfoils (ONERA) have been built in transonic wind tunnel environments. The most disruptive and recent gust generator was built by ARA [7] and uses a network of solenoid valves (1800 fluid actuators mounted on two fixed profiles) to make rapid changes to the tunnel flow direction.

In general, the criterion used to assess gust generator performances is the ratio between vertical and longitudinal velocities of the flow in the WT test section. This ratio is called “gust angle” or “gust amplitude” is mentioned many times in this document and refers as the value in degrees of

$$A_{gust}(t) = atan\left(\frac{V_z(t)}{V_x(t)}\right)$$

Within the framework of CS1 SFWA-ITD, the first version of gust generator concept consisted in two identical airfoils installed upstream of the wind tunnel test section. The dynamic pitch oscillations allowed to produce air flow deflections leading to the generation of a cylindrical gust field downstream. The exploitation of this first device fulfilled the initial requirements and specifications: the gust generation process has been controlled and is efficient enough to generate unsteady fluctuations of vertical velocity and to induce aerodynamic and aeroelastic effects on a model. But within the framework of CS2 Airframe-ITD, the main objective is to dispose of a device allowing larger flow deviations. The ambition is to generate gust waves with targeted figures:

- a gust angle amplitude of $\pm 1^\circ$ in the model area,
- a frequency bandwidth up to 100 Hz,
- operating conditions in transonic flow conditions (Mach number ~ 0.82).

2.2 A simplified model of the Gust Generator

In order to investigate the improvement capabilities of the existing gust generator, a simplified model was used. Based on the formulations described in [5] and [6], theoretical analyses were performed to study the influence of the main parameters and to identify the improvements axes of the existing test setup. Accordingly, the gust angle that can be generated by the existing 2 oscillating airfoils, can be formulated as

$$A_{gust} \sim \beta A_{motion} \frac{dC_L}{dA_{motion}} \cdot |C(St)| \cdot \frac{f_{motion} \cdot c}{U_0} \cdot R\left(\frac{H}{c} St\right)$$

with A_{motion} and f_{motion} the amplitude and frequency of the dynamic pitch oscillation,

$\beta = 1/\sqrt{1 - M^2}$ the compressibility and speed effects of the flow at Mach number M , and U_0 the streamwise velocity,

St the Strouhal Number and $C()$ the Theodorsen lift-deficiency function,

c the airfoil chord and $\frac{dC_L}{dA_{motion}}$ the lift coefficient derivative,

$R(-)$ a function depending on the gust generator geometry (chord c), the WT upper and lower walls (height H) and the Strouhal number.

This relation is important as it shows the dominant parameters. The gust amplitude linearly depends on the pitch amplitude of the airfoils and evolves with the frequency (or Strouhal number) in a way that is determined by a linear law modulated by the Theodorsen's correction. The influence of the walls deteriorates the gust generation capabilities especially for low frequency (i.e., large gust wavelengths) [6].

In order to dispose of a test rig to be implemented in the S3Ch facility and allowing larger flow deviations, the first idea was to influence the dynamic circulation around airfoils driven by the dynamic motion (through the parameters $A_{motion} \frac{dC_L}{dA_{motion}}$) with an active flow control technology driven by pulsed blowing (similarly through the parameters $Q_{mass\ flow} \frac{dC_L}{dQ_{mass\ flow}}$, Q being the mass flow rate) [7] [8].

3 GUST GENERATION CONCEPTS DOWN SELECTION AND PARAMETRIC ANALYSES

3.1 Preliminary investigations and selected approach

In the preliminary phases, a feasibility study based on numerical simulations was performed by ONERA with the high-fidelity elsA software to explore the ability of active flow control technologies. A promising concept was derived and composed of airfoils combining dynamic pitch oscillations and unsteady blowing slots.

All data and insights were used in the works achieved by the GUDGET Consortium partners within the objective to derive an optimal gust generation concept using a general numerical approach. Preliminary loads calculation and mechanical feasibility studies have been performed considering several criteria such as mechanical strength, mass and inertia constraints, available space, considerations on dynamic motion performances, fluidic flow rate performances ... At the end, the possibility to implement vane movement and jet actuation simultaneously has been discarded for the unfeasible actuation of highly loaded vanes at high frequency, with the high vane mass resulting from the installation of the fluidic actuators. As a main result, the impossibility to design an optimal hybrid concept led to the decision to implement two separated systems for gust generation that operate in a specific frequency bandwidth:

- A moving vanes gust generator for the low frequency range [0-50] Hz. This concept is fully based on the previous one, with a major improvement, namely by introducing a flapping control surface, where the airfoil and flap are moved synchronously.
- A fixed vanes gust generator with fluidic pulsed jets for the high frequency range [50-100] Hz. This concept uses fluidic actuators to produce precise bidimensional sonic jets through blowing slots located on upper and lower sides on each airfoil next to the trailing edge.

For each system, numerical simulations have been achieved to design optimal solutions with trade-offs between gust generation performances and design constraints. CFD simulations were carried out by GUDGET Consortium partners by utilizing the TAU-Code for both RANS and URANS simulations especially in the transonic range for a Mach number of 0.82.

3.2 The computational domain and the baseline configuration

For the optimization and design processes of both gust generator concepts, the existing ONERA gust generator architecture [4] was considered as the baseline configuration. Figure 2 shows the computational domain considered for the CFD computations needed to properly collect the performance and the aerodynamic data to perform the design analysis. The computational domain consists of a section of the S3Ch wind tunnel with two vanes, whose chord length is, initially equal to 200mm located at a distance of 3500 mm from the inlet section of the convergent duct and just before the test chamber. The baseline airfoil is a NACA 0012. The airfoil, together with the points where the gust angle magnitudes for performance evaluation are taken (indicated as x_1 , x_2 , and x_3), are shown in Figure 2.

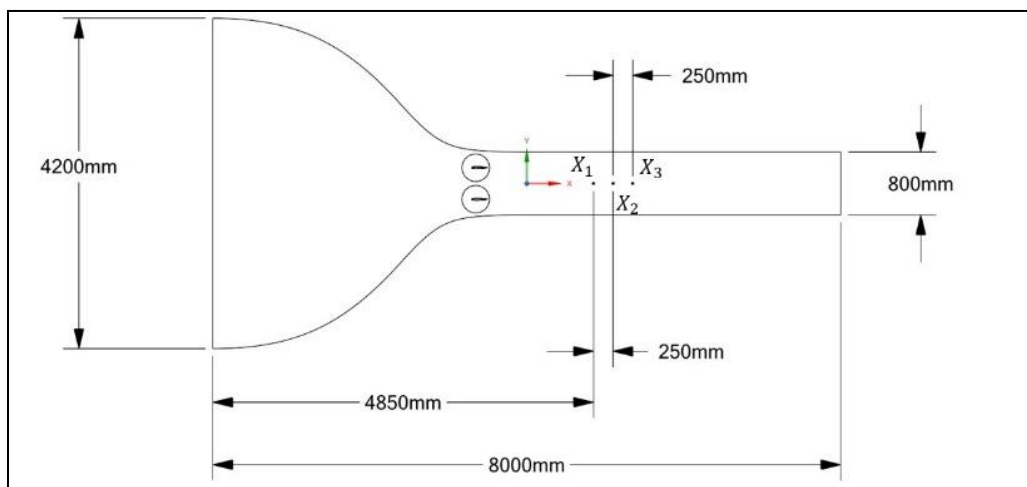


Figure 2 : General layout of CFD modelling

3.3 Airfoil design optimization

Among all the functioning parameters, the optimization of the airfoil for both movable and fixed vanes play an important role in the gust generation capabilities. The design space has been chosen considering also mechanical design related aspects, such as the need to have a thickness as high as possible, especially in the trailing edge area of fixed vanes concept. The optimization process has been performed through a series of unsteady RANS analyses and has been carried out by using Design of Experiment (DOE) method along with response surface technique as reported in [9].

Starting from the NACA 0012 airfoil typically adopted for the design of gust generators, process aimed at generating a modified NACA 4-Digit symmetric airfoil. Airfoil geometry has been parametrized considering three major design parameters: leading edge radius (l), chordwise position of maximum thickness (T - in tenths of chord) and maximum thickness (t). The output (performance) parameter was the maximum gust angle.

For movable vanes, the optimization process led to a final geometry which increased significantly the baseline performances without losing in maximum thickness. The response surface generated based on the computed performances is shown in Figure 3. A zone which corresponds to the high-

performance designs can be clearly identified, which leads a gain in terms of maximum gust angle higher than 15 % (by comparing with the red point indicating the baseline performances).

For the fixed vanes, the simulations have shown two zones of high-performance output are clearly identified, but the improvement in changing the shape is not as strong as the one obtained for the movable vanes.

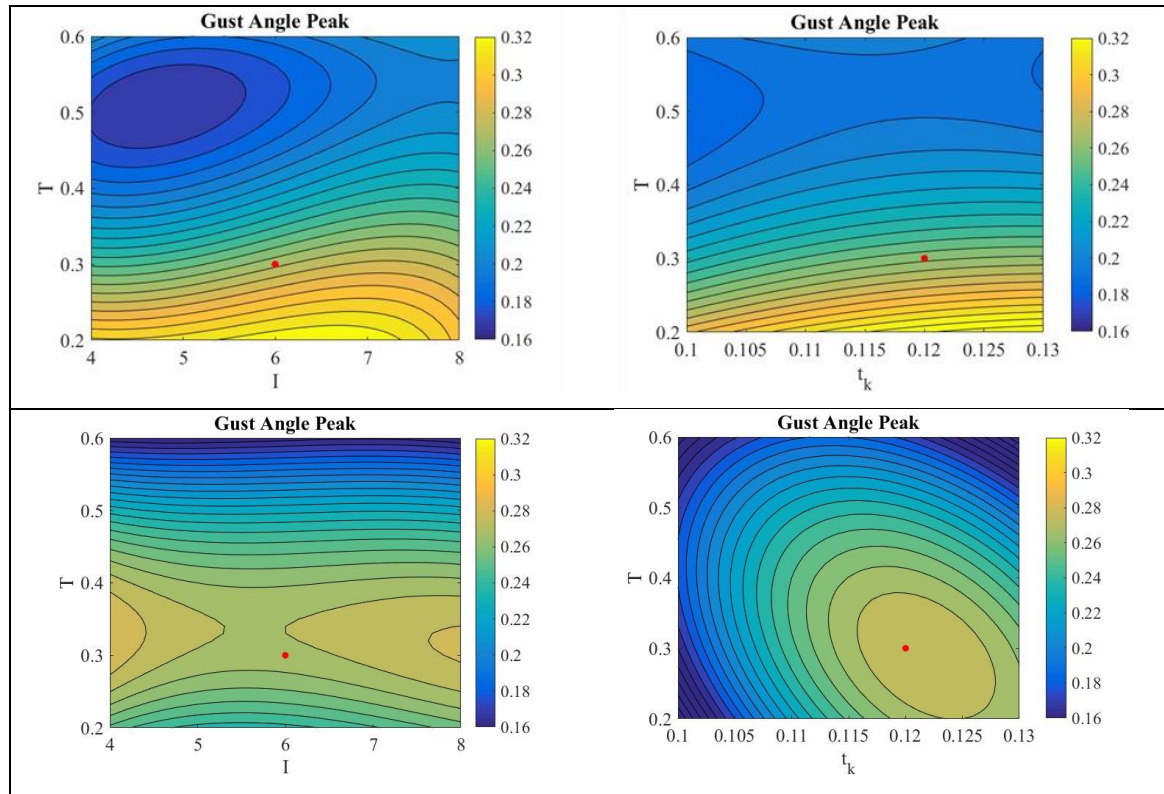


Figure 3 : DOE Response surface for the optimisation process for the movable vanes (top) and fixed vanes with pulsed slot (down) – Colorbar gives the gust angle scale

3.4 Parametric study of the movable vanes concept

The concept of the movable vanes is based on the gust generator previously design and tested by ONERA [4]. The radical idea is to add on the pitching airfoil a flapping control surface, where the main airfoil and the flap are synchronously and harmonically moved around a hinge line located at 75% of the airfoil chord.

CFD simulations assessed the effects of geometrical and actuating parameters on gust generation performances. Typical results are illustrated in Figure 4 presenting instantaneous snapshots of the flow field around the 2 oscillating airfoils.

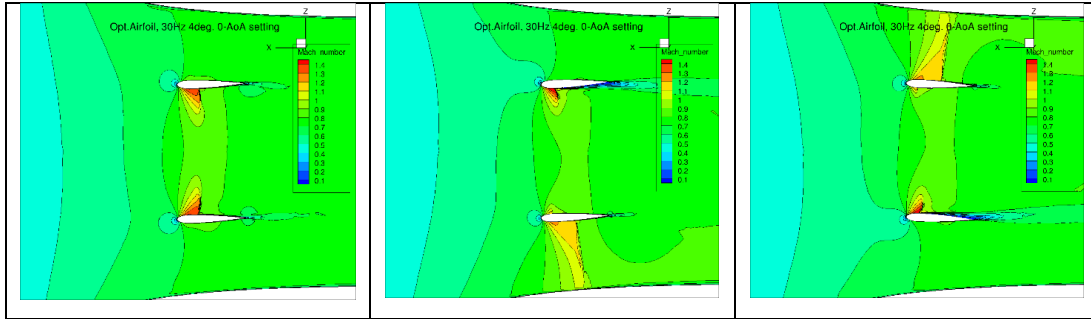


Figure 4 : Instantaneous flow field around vanes (plain optimized airfoil, $M = 0.82$, 0-AoA setting)

Figure 5 shows quantitatively that the flapped vanes provide a better performance than the plain vanes while maintaining a similar trend over frequencies. Referring to theoretical model [5] [6], the effect of additional flap rotation produces more extended recirculating zones in the rear part of the airfoil compared to the plain airfoil configuration. As a consequence, the gust angle distribution for the flapped configuration allows to generate higher gust angles in the test section. An extended list of parameters was tested numerically through CFD such as the frequency and amplitude of motion, the steady vanes inclination, the airfoil chord length, the distance between the 2 vanes ...

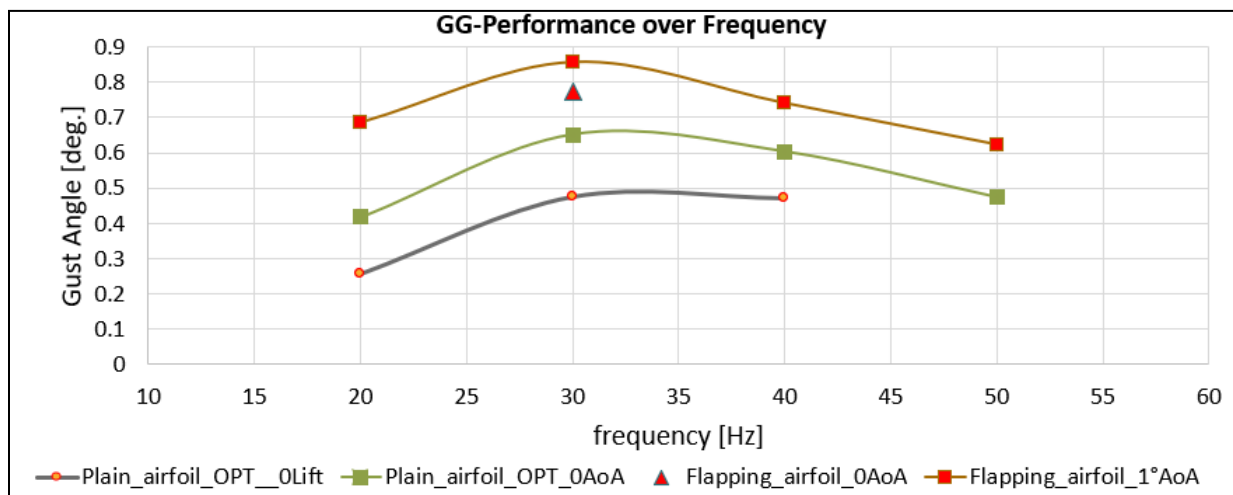


Figure 5 : Movable vanes, performance over frequency, comparison of different configurations

3.5 Parametric study of the fixed vanes concept with pulsed blowing slots

As the motion amplitude is a key parameter for the movable vanes concept, the fluidic mass flow rate is relevant for the fluidic gust generator concept. For the design of the fixed vanes plus the fluidic jets, several parameters have been investigated by considering a mass flow generated by the fluidic actuator equal to 120 g/m/s driven harmonically by the pulsed blowing frequency.

Based on the optimised airfoil, parametric CFD simulations have been performed including several parameters such as the variation of the setting of the vane inclination, the jet location or the forward inclined jet angles. Typical results are illustrated in Figure 6 presenting the flow in the vicinity of the blowing slot and the gust field in the WT test section downstream the gust generator.

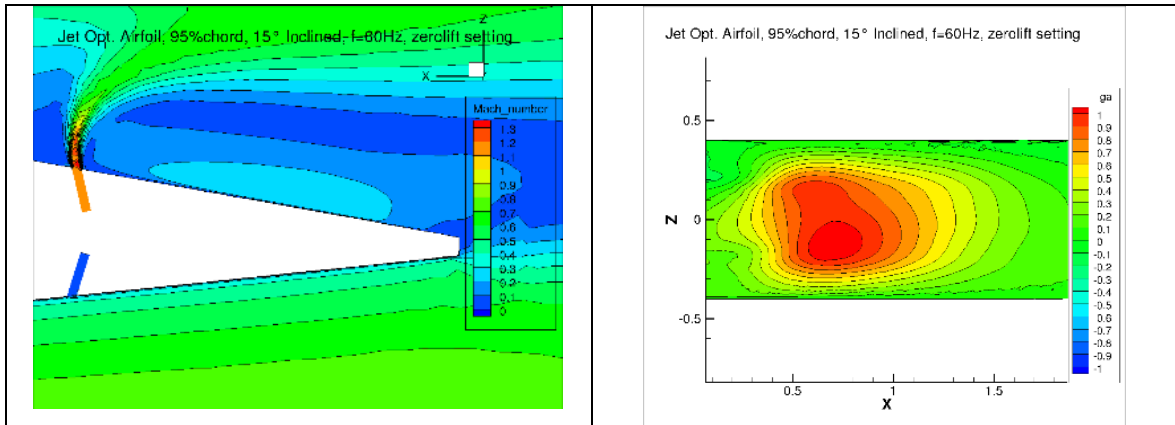


Figure 6 : Fixed vanes with pulsed slots : detail of Mach number distribution close to the slot (left) and Instantaneous gust angle distributions inside the test section (right)

Figure 7 shows quantitatively the performance of fixed vanes with the pulsed blowing slots against various configurations or parameters. It is apparent that higher pulsed jet frequencies produce higher performances in terms of gust angle. Moreover, a jet inclination of 15° increases the performance significantly, if compared with the perfectly vertical jet or other angle values. Besides, the gust angle performance decreases as the jet slot location is moving forward on the airfoil chord. Additional investigations have also been performed e.g. by adjusting the vanes inclination setting or by varying the airfoil chord length.

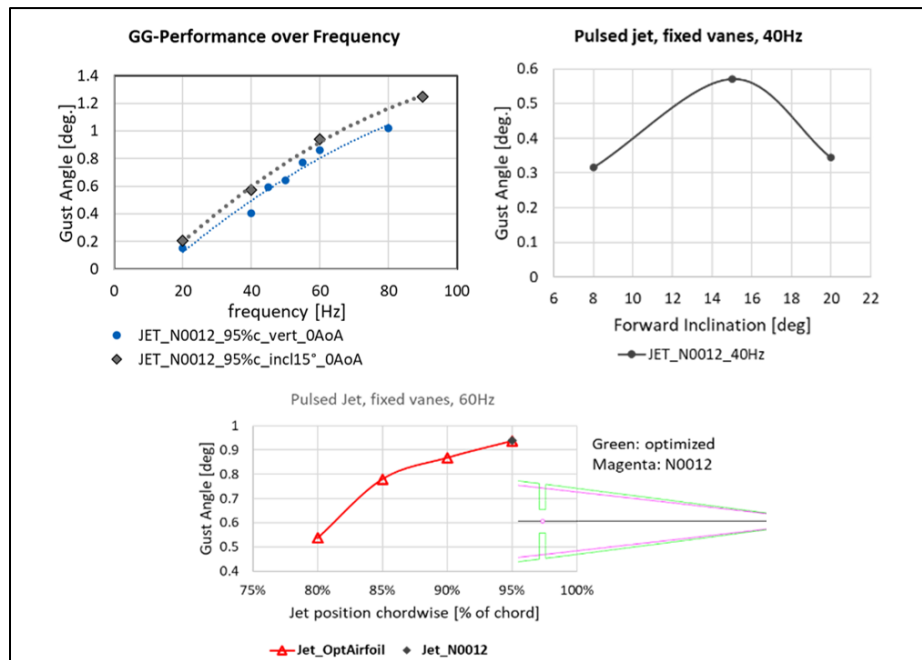


Figure 7 : Sensitivity of gust generation performances against various design parameters

3.6 Summary of Gust Generation performances

An extensive design process has been performed with numerical simulations to design optimal solutions with trade-offs between gust generation performances and design constraints.

The performances of gust generation systems are summarized in Figure 4 for a Mach number of 0.82 in the S3Ch facility.

For the low frequency domain system, the theoretical target of 1° of gust amplitude is not strictly attained in the range [0-50] Hz but is close to 0.8°, these updated figures have been deemed acceptable since it represents an improvement with a factor larger than 2, in terms of gust generation capability, with respect to previous wind tunnel test results. For the higher frequency domain system, the theoretical performances are good enough to reach the target of a gust amplitude of +/- 1° in the range [50-100] Hz and to overcome it for frequencies higher than 60 Hz.

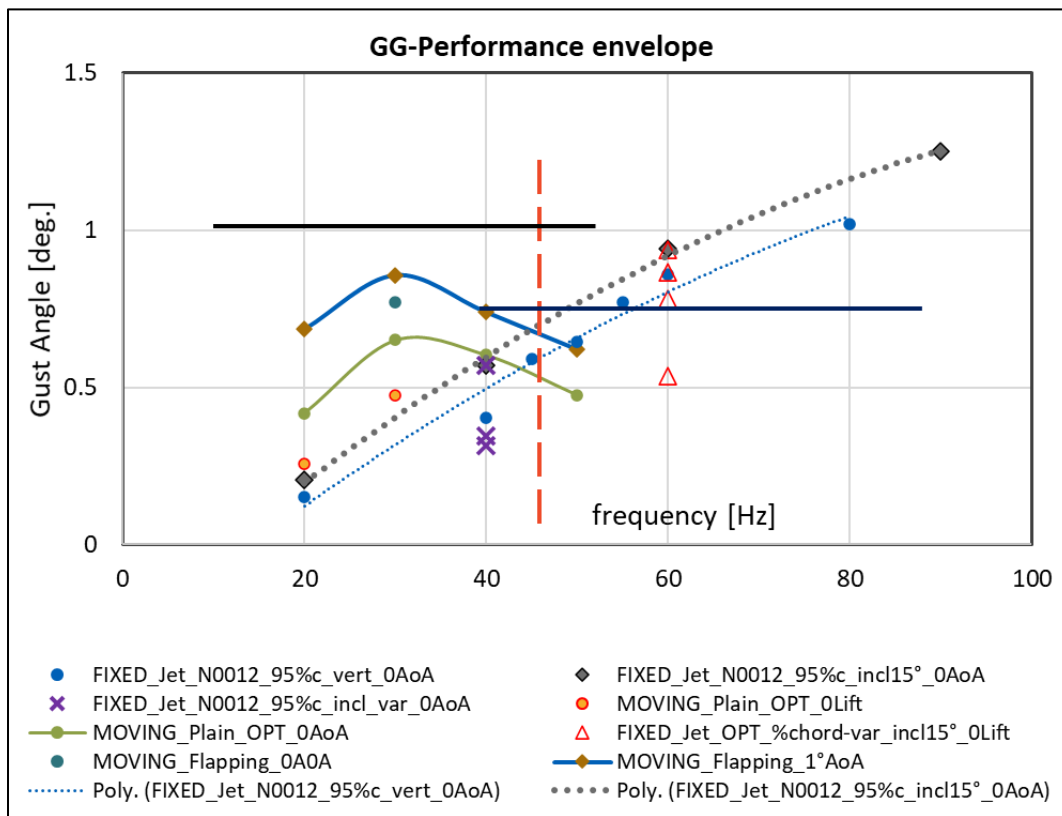


Figure 8 : Summary of the numerical simulations results of the “optimised” gust generation devices (gust amplitude versus gust frequency for several concepts configurations)

4 DESIGN AND MANUFACTURING OF THE GUST GENERATION DEVICES

4.1 General arrangements

The gust generators concepts have been developed to be installed and operated in the S3Ch transonic wind tunnel facility, both fixed and movable vanes systems mounted on specific structural supports connected to the lateral walls of the convergent section, suitably modified to allow for quick installation and deinstallation. During the extensive design process, a large effort has been performed by the GUDGET Consortium through structural analyses (i.e., modal, stress and fatigue ...) according to the ONERA WTT model sizing rules.

The two interchangeable systems, i.e. fixed vanes equipped with fluidic actuators and flapped movable vanes, are described in the next subsections.

4.2 Movable flapped vanes gust generator

The system is composed of two identical vanes to be implemented in the WT facility, an upper and a lower vane. To divert the airflow and generate a gust, each movable vane oscillates around the main spar rotational axis and is supported by roller bearings on both sides and connected on the wind tunnel walls.

The structure is a hybrid metal-composite structure, with a main spar made of steel and directly connected to the oscillation actuation, vane panels are made of CFRP composite, and ribs made with a CFRP-foam sandwich. The rear spar, made of aluminium, is equipped with hinges to be connected with the flap. The flap is a full CFRP structure, with a spar running all along the flap, connected to the main vane body by means of hinges and ball bearings.

Deflecting the flap simultaneously to the main vane (rotating about the hinge axis - Figure 9), increments the lift coefficient of the whole vane, increasing the generated gust effect. Levers on both sides of the flap are connected to a mechanism (Figure 10), providing the possibility to change the ratio between flap deflection and main vane deflection with respect to the reference position.

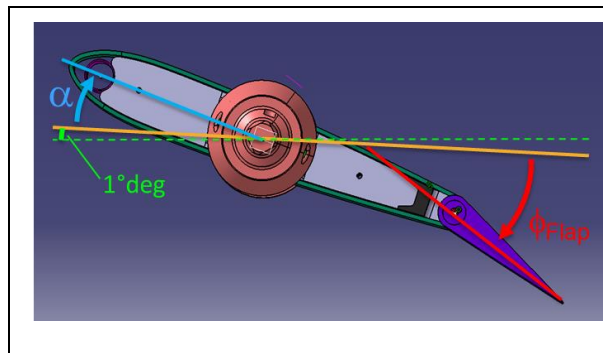


Figure 9 : General arrangement of the fixed vanes system

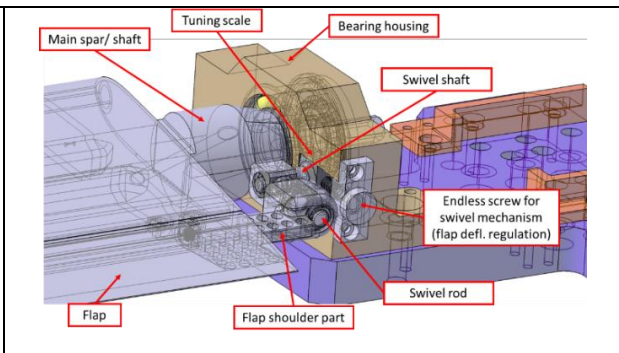


Figure 10 : Movable vane, flap actuation mechanism

The actuation is performed by four servohydraulic jacks which synchronously rotate the two airfoils. Each airfoil is driven at its two sides and each high torque - high speed actuator is composed of a rotative hydraulic actuator operating at 200 bar using a fast response servo valve and a rotary position sensor. The actuation device includes a security system that stops the

actuation whenever the two roots of one airfoil are not at the same angular position, thus preventing any unwanted torsional deformation of the airfoils. Position feedback control laws are precisely tuned to allow the dynamic deflection over a wide frequency bandwidth (i.e. up to about 100Hz), with a classical pitch amplitude decreasing as the frequency increases.

The movable flapped vanes gust generator is illustrated in Figure 11 during the laboratory tests to assess its dynamic functioning and performances.



Figure 11 : Laboratory characterisation of the movable flapped vanes gust generator

4.3 Fixed vanes Gust Generator with pulsed blowing slots

The fixed vanes system is one of the two gust generator variants to be used for the high frequency gust generation by deflecting the flow via fluidic actuators producing precise high frequency bi-dimensional sonic jets.

The static vanes are designed to house fluidic Pulsed Jet Actuators (PJA - Figure 12) as well as routing airflow to and from them within the confines of an aerodynamic airfoil. The concept of PJA was developed in a previous project (see [10] for more details) and allows to design high performances valve for active flow control (high air exit velocity, high mass flow rate, high actuation frequency [11]). For the present case, the main specification was to have a mass flow rate of 128 g/s for each vane in order to create a sonic jet in each slot. Practically, for each vane, the final solution is composed of 4 PJA with a mass flow rate of 32 g/s and supplied with an upstream pressure of 10 Bar. Each PJA embeds 2 amplified piezoelectric actuators working as valves and remote control in order to rout the internal flow alternatively to the lower and upper slots.

The PJAs, installed inside the static vanes, suitably secured to the vane structure, generate pulsed jets out of circular nozzles. Internal channels are used to direct the airflow from PJAs' outlets to bi-dimensional slots located close to the trailing edge, in both upper and lower sides of the vane. Alternative flows from upper and lower sides create an oscillatory flow deviation which generate the gust inside the test section.

Four PJA fluidic actuators fit alongside the vane span in each vane: each PJA is equipped with two inputs providing the operating pressure and two sets of six outputs, each set being operated individually and feeding in turn the pneumatic channels routing the air either on upper or lower side of the vane. Figure 13 shows a sketch of this arrangement.



Figure 12 : first PJA prototype

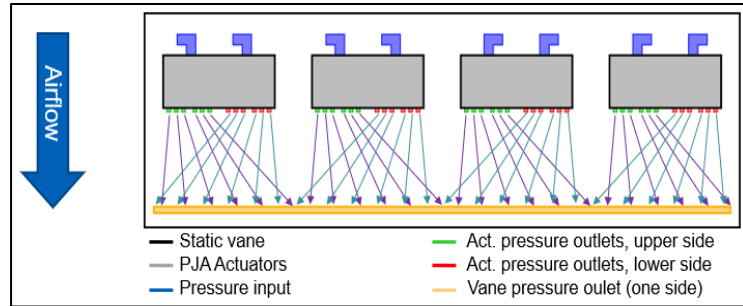


Figure 13 : Sketch of PJAs arrangement inside each static vane

The distribution of the flow from the circular outlets of the PJAs to the rear slot requires internal channels of complex geometry. One of the most peculiar features is that, to cover the full width of the outlet, the internal channels of the top and bottom sides need to cross over one another without interference. The geometry shown in Figure 14 has been designed by CFD computations to enable uniform mass flow rate at the outlet of the six channels - Figure 15 from [9].

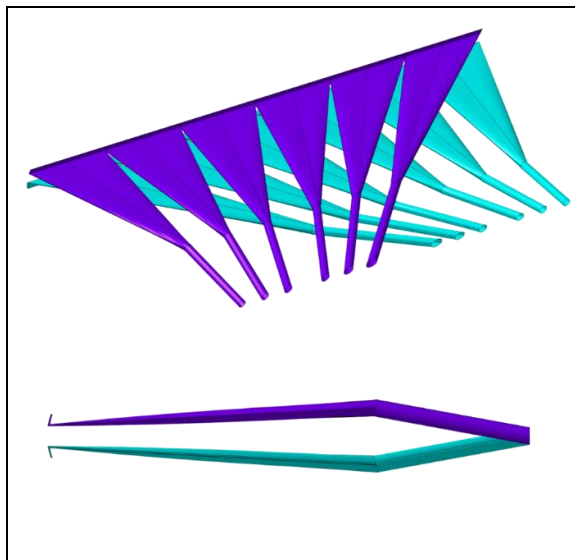


Figure 14 : Overview of the geometry of the internal channels, isometric (Top) and side view (Bottom)

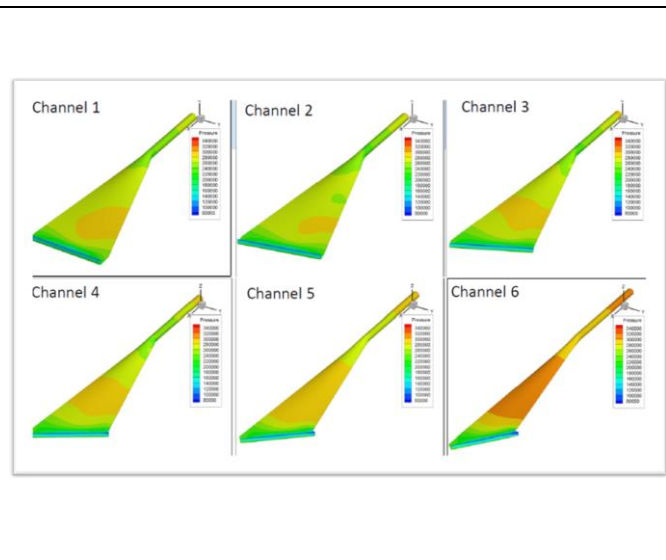


Figure 15 : CFD RANS computations on internal channels of the fixed vanes

The channels are separated, from a mechanical design point of view, into two halves, one side belonging to the main body and the opposite side shaped in the inner side of the trailing edge

covers. PJAs are installed inside the static vanes in several pockets and are protected by two covers located at the leading edge of the vane airfoil. The lower edge of the cover implements a gap which defines the vane outlet slot.

A set of large pressure tubes feed the PJAs with pressurised air. These tubes are routed inside the model from both sides and run through a channel in the leading-edge. In the same compartment, electrical wires and connections are routed up to the PJAs for internal measurement and control. The manufactured and instrumented final arrangement of the fixed vanes gust generator (without the leading edge covers) is shown in Figure 16. Each vane is made of five main metallic parts (main body, two trailing-edge covers, two leading-edge covers) in addition to the PJA devices.

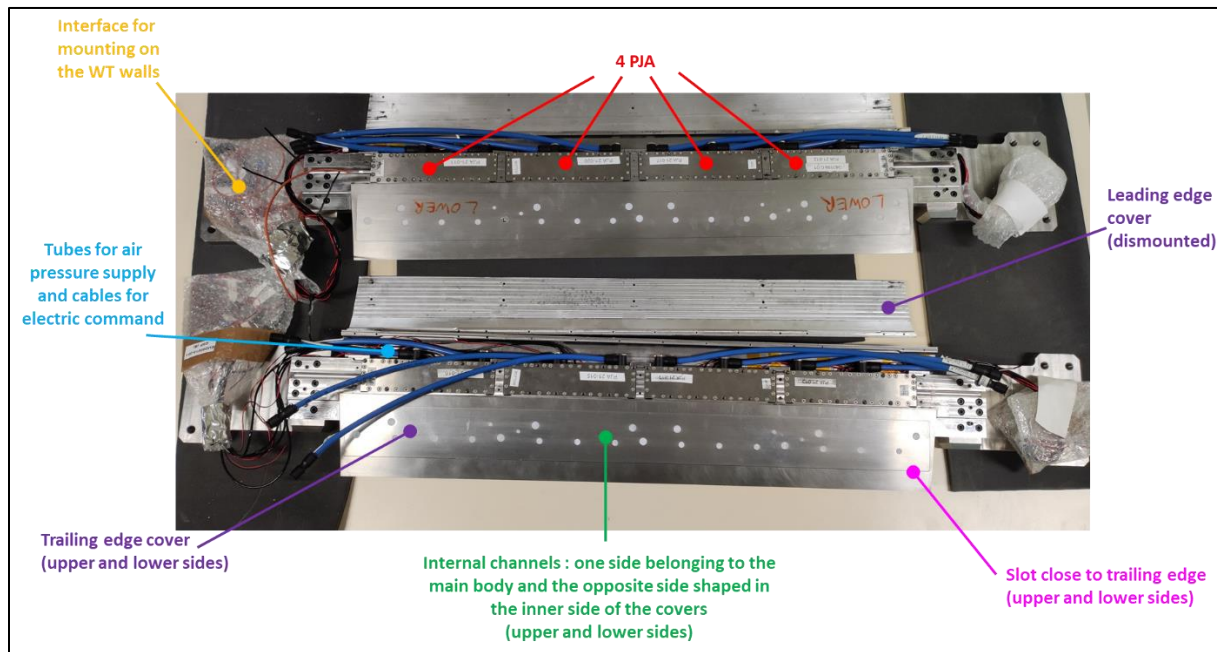


Figure 16 : Overview of the 2 fixed vanes gust generator

5 WTT CHARACTERISATION OF GUST GENERATION DEVICES

5.1 WT facility and gust generation devices assessment

The WTT campaign was carried out in the research ONERA S3Ch Wind Tunnel located in the ONERA Meudon Centre. This facility is powered by a 3500 kW two-stage motor-ventilator group, equipped with 24 blades, which rotate at a fixed rotational speed of 1500 rpm. The test section size is 0.76 m × 0.804 m × 2.2 m. The Mach number domain extends from 0.3 to 1.2. The stagnation pressure is the atmospheric one, and the stagnation temperature lies between 290 and 310 K. The shapes of the upper and lower walls can be either rigid or deformable adaptive. In the latter case, the walls are adapted for each flow condition based on a steady flow hypothesis so as to reproduce far-field conditions by minimizing the wall interferences. The flow velocity is adjusted by a downstream sonic throat, which warrants a $\pm 10^{-4}$ uncertainty of the Mach number value.

The goal of the first part of the test campaign was to assess the performances of the improved gust generation devices, designed and manufactured within the GUDGET Consortium. Tests have been conducted to investigate the unsteady flow field downstream the gust generators in the test section for different aerodynamic conditions and for different driving commands. The measurements were based on an unsteady clinometric probe designed specifically for these types of measurements. A preliminary calibration phase of the probe was achieved in the Wind Tunnel test section for a wide range of flow conditions. An overview of the clinometric probe mounted on its support in the WT test section is illustrated in Figure 17. Once the probe has been calibrated and the acquisition parameters set, the measurements provide a real-time evaluation of the so-called gust angle.

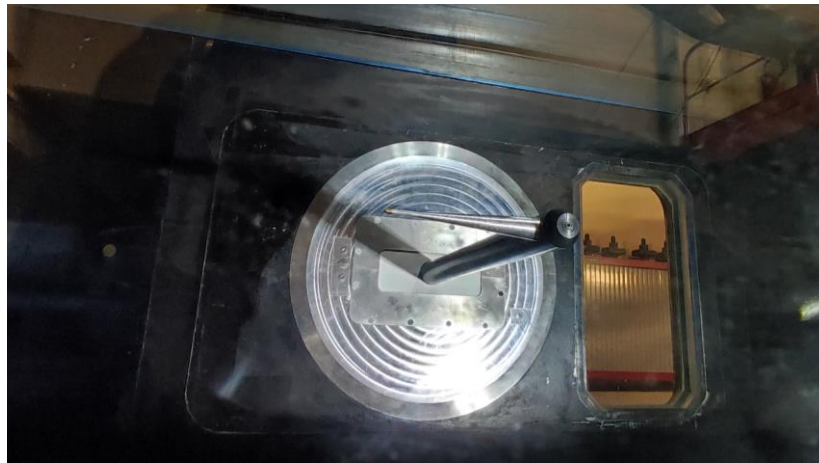


Figure 17 : Unsteady clinometric probe for the assessment of gust generation performances

5.2 Fixed vanes Gust Generator with pulsed blowing slots

This device was directly tested in the wind tunnel environment. Indeed, as it is based on pneumatic supply with significant pressure and mass flow rate requirements, it was not possible to evaluate its performance in the laboratory. At the S3Ch facility, a specific pressurized air supply line was designed and manufactured by ONERA to expand the air compressed at 250 bars to the required pressure level of 10 bars while ensuring the total required mass flow rate of 256g/s. A picture of the final part of the pressured air flow line test setup is illustrated on the top left side of Figure 18. The compressed air is supplied on each side of the two profiles by several pneumatic lines. The gust generator installed in S3Ch facility is shown at the bottom side, suitably connected to the lateral walls of the final part of the WT convergent.



Figure 18 : Fixed vanes gust generator installed in the final part of the wind tunnel convergent section (bottom) – Mounting part and pneumatic supply line (top)

Typical results are shown in the next figures presenting temporal evolutions of the "gust signal" for a harmonic oscillation of the gust generator. As expected, a unique command induced a sinusoidal dynamic motion of the PJA actuator distributed in each vane. As a result, a pulsed blow is generated alternatively in the upper and lower slots and synchronously for the 2 vanes. The functioning is clearly depicted in Figure 19. The PJA actuators were equipped with strain gauges providing a feedback information on the dynamic motion of the vanes. Whatever the frequency, the vanes operated perfectly in phase: the actuators supplying the same slot (upper or lower side) operated synchronously and the functioning of the 2 airfoils is perfectly in phase.

A sinusoidal command of fixed vanes gust generator induced a periodic gust downstream in test section. As anticipated in the design phase, the gust generator efficiency is targeted for the high frequency bandwidth. For low frequencies, the signal to noise ratio of the probe signal is very low and masked by the turbulent noise of the flow. For higher frequencies, the probe signal quality is clearly improved. A frequency analysis of the gust signal indicated that the principal component of the gust field is located on the command frequency. Higher harmonics could be identified but with a lower order of magnitude.

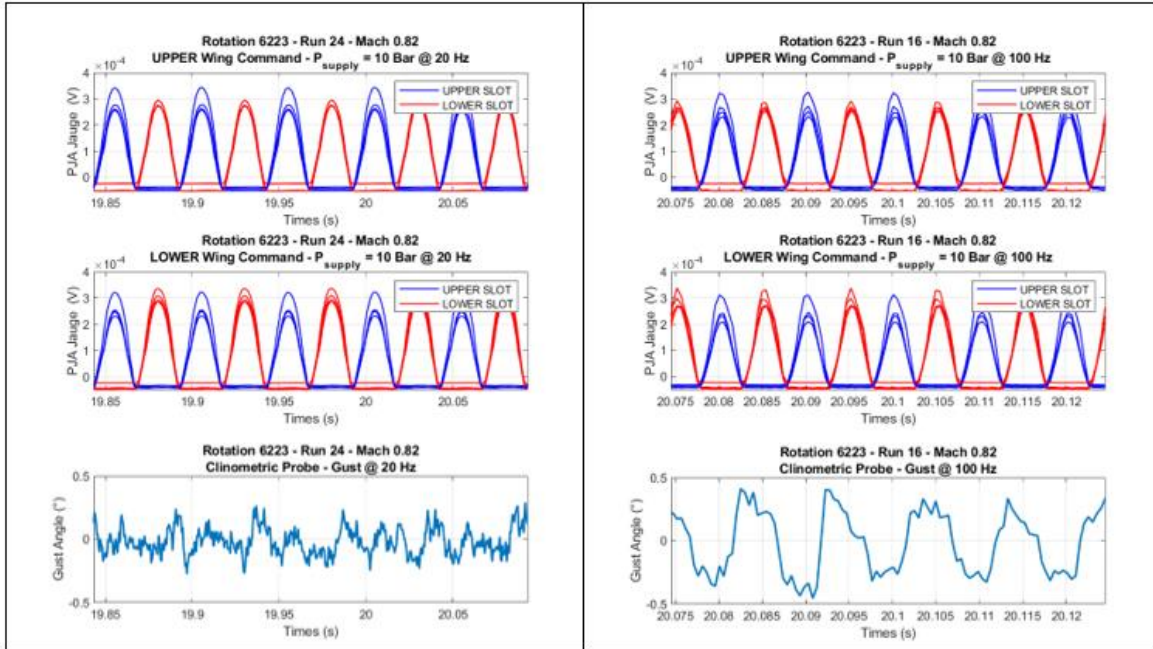


Figure 19 : Temporal evolution of Gust Generator Commands and Clinometric Probe Signal for tests at Mach = 0.82 and $P_{supply} = 10$ Bar

Figure 20 illustrates the influence of the frequency on the gust generation capabilities, at fixed Mach number and fixed supplied pressure, and for sine or sweep signal commands of the set of PJA. The gust amplitude is quasi linearly dependent of the frequency command signal as expected in the theoretical or numerical performances predictions. The pressure level supplied to the PJA has also a proportional effect on the resulting gust amplitude. For identical frequency command of the driving signal, the greater the pressure level, the greater gust amplitude is. The increase of the Mach number limited the gust amplitude generated by the fluidic generation device: as the longitudinal flow velocity increases, the velocity ratio decreases, limiting the gust amplitude. Moreover, the increase of the Mach number clearly deteriorates the signal to noise ratio of gust because of the growth of the turbulent noise.

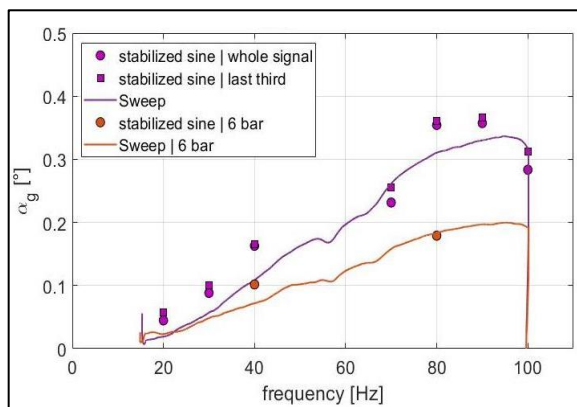


Figure 20 : Frequency and Supplied pressure level effects (purple = 10 bar and orange = 6 bar) on the Gust amplitude for Mach = 0.82

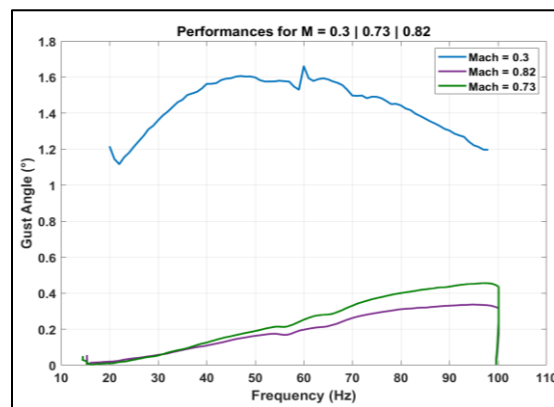


Figure 21 : Wind Tunnel Flow velocity effect on the Gust amplitude for $P_{supply} = 10$

5.3 Movable flapped vanes gust generator

The installation of the movable flapped vanes gust generator in the S3Ch facility is shown in the right part of Figure 22. The left set of dynamic actuator devices (servo-hydraulic actuators, fast servovalves, motion sensors, hydraulic pressure supplier line) are presented in the left part of Figure 22.

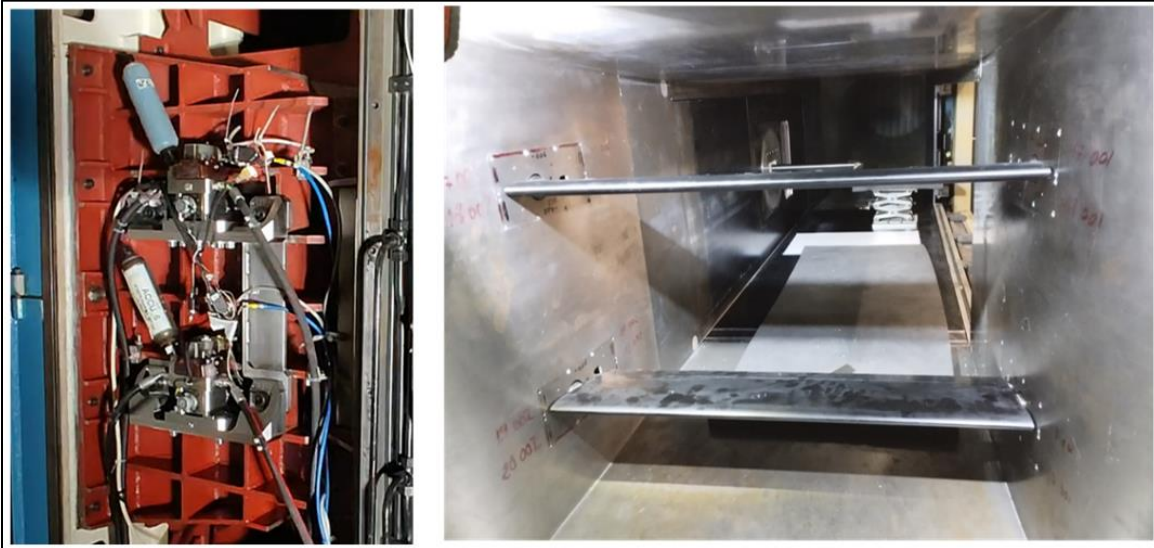


Figure 22 : Movable flapped vanes gust generator installed in the final part of the wind tunnel convergent section (right part) – Mounting part and hydraulic actuation components (left part)

As shown in Figure 23, a sinusoidal command induced a sinusoidal dynamic motion of the 2 vanes, hence generating a sinusoidal gust. For this example, at Mach number 0.3, a dynamic flaps deflection of $\pm 4^\circ$ in addition to a dynamic pitch oscillation of the vanes of $\pm 4^\circ$ at 20Hz, induced a gust amplitude recorded by the probe of about $\pm 1.22^\circ$ flow deviations. A frequency analysis of the gust signal indicated that the principal component of the gust energy is located at the command frequency. As depicted in Figure 23, the signal to noise ratio of the gust angle is very good. Higher harmonics could be identified but with a lower order of magnitude.

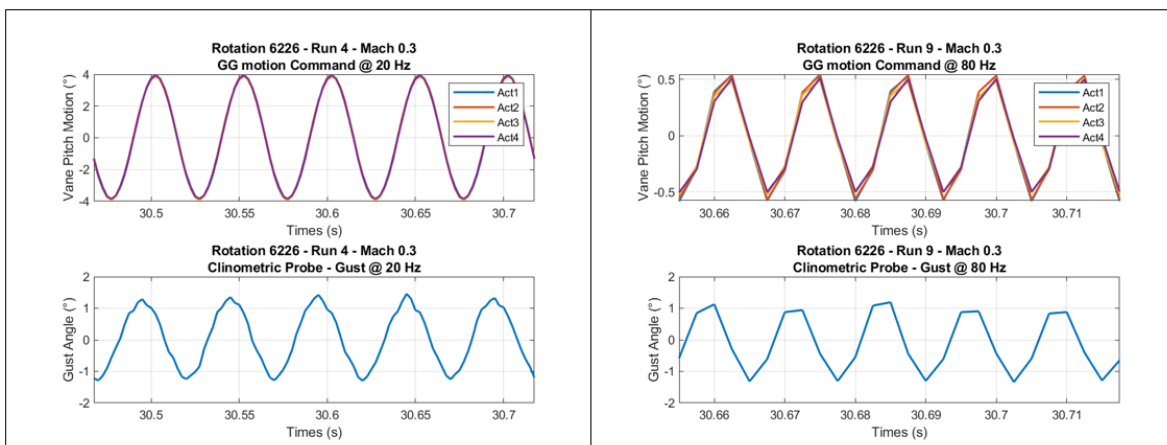


Figure 23 : Temporal evolution of pitch motion and Clinometric probe signal for Mach = 0.30

Typical results of the movable flapped vanes gust generator are summarized in Figure 24, presenting the gust angle amplitude for different signal parameters (motion frequency and amplitude) driving the dynamic motions of the flapped vanes. The evolution of the gust amplitude is modulated by the actuators dynamic performances in addition to other factors (loads, electrohydraulic position control, aerodynamic efficiency ...). The results, for Mach number of 0.3, indicated very good performances in terms of gust generation with gust amplitude up to $\pm 2^\circ$ illustrating an improvement with respect to the previous gust generation apparatus developed within CS1-SFWA ITD.

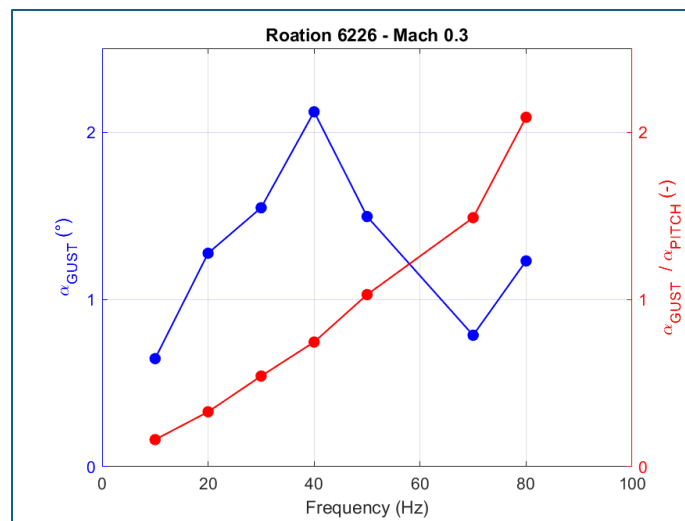


Figure 24 : Typical results of Movable flapped vanes gust generator for Mach = 0.3 (driving signal Frequency effect)

After the tests in the low subsonic range, the flow velocity was increased to reach the transonic regime. During the Mach number increase, a very strong and sudden instability occurred on the experimental setup. After the emergency stop, the inspection of the assembly revealed damage on the lower vane due to severe friction of the flap on the wind tunnel walls. Without any measurements taken during this transient phase, no clear explanation could be found for the phenomenon (aeroelastic flutter instability, hydraulic servo instability, aerodynamic flow instability, etc ...).

5.4 Conclusion on the new gust generation devices

A summary of the objectives, the design predictions and the corresponding WTT characterization results of the gust generation capabilities is presented in Figure 25 for the most critical aerodynamic flow conditions (i.e. Mach number = 0.82):

Fixed vanes gust generator with pulsed blowing slots

The characterization of the fluidic concept for gust generation has shown a great potential in terms of use and operation. The fixed vanes gust generator with pulsed blowing slots is easy to operate in a wind tunnel environment. It allows to command remotely 16 pneumatic supply channels,

either fully coupled or independently, which drive the dynamic blows in the slots located on the lower and upper surface of each vanes.

As expected, the quality of the gust signals clearly indicates that this device is better suited to high frequencies than low ones. Further investigation of the two-dimensional gust field would be interesting, but was not possible due to time constraints on the WTT program.

On one hand, the parametric effects on gust-generating capability depend, as expected, of various parameters such as the frequency of the driving signal, the supply pressure, or the WT flow velocity. On the other hand, the overall performances of the gust generator are significantly below forecasts, predicted during the design phase and based on numerical simulations. As illustrated in Figure 25, the difference between predictions (**green curve**) and tests (**pink curve**) is characterised by an “inefficiency ratio” close to 4 over the frequency bandwidth. Some analyses are still under investigations to understand these discrepancies.

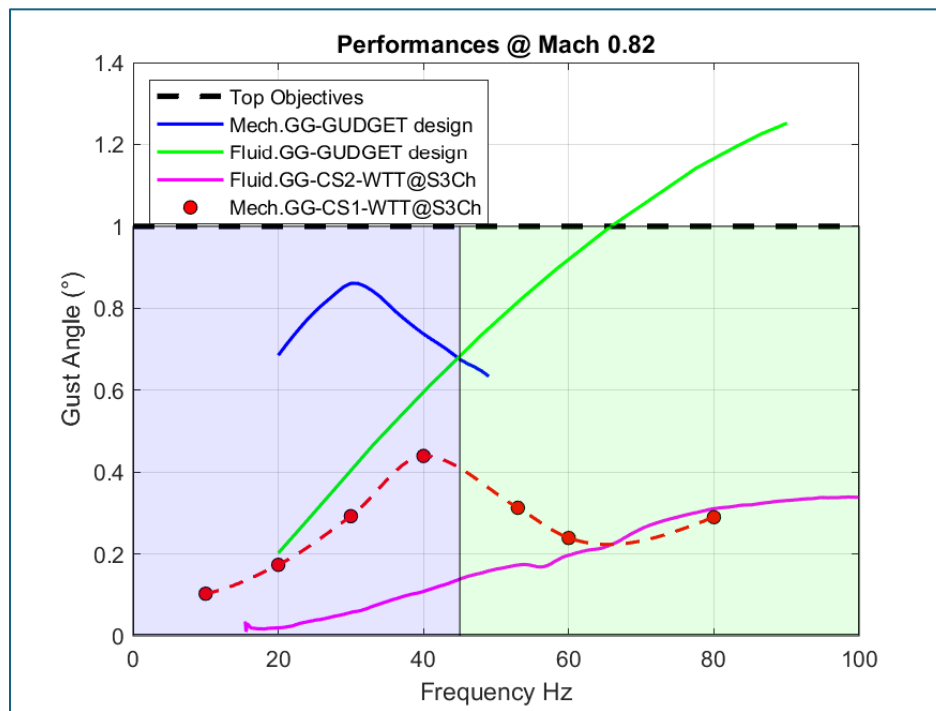


Figure 25 : Summary of results: specifications, simulations and tests @ Mach = 0.82

Movable flapped vanes gust generator

After adjustments and settings, required after the laboratory characterization, the movable flapped gust generator proved to be, also, very easy to use in a wind tunnel environment. The performances obtained at Mach 0.3 are greater than the one obtained in previous tests [4] based on the gust generator with dynamically oscillating wings in pitch (only). However, the incident that occurred during the WTT, did not allow to assess the gust generation performances in the transonic domain and to verify the design predictions (**blue curve**).

After the instability occurrence and damages on the lower vane, the device was analysed and repaired by the GUDGET partners. However, for scheduling reasons and risk management, this

gust generator concept could not be tested again in the S3Ch wind tunnel. Priority was given to continuing the tests on the mock-up described [12].

Conclusion on the new gust generation devices

Both gust generators developed within the GUDGET consortium have shown a significant potential in terms of operability and parametric command. However, due to limited performances, particularly in highly loaded and complex flows in the transonic regime, it was decided to reuse the gust generator developed in the framework of Clean Sky 1 SFWA ITD [4]. This well-known and mastered gust generation device already proved to be effective (**red curve**) and robust, and has been reinstalled in the S3Ch facility.

The two gust generation concepts (both fluidic and mechanical concepts) remain very promising for applications and tests in wind tunnel environment and could be investigated in future research programs.

6 DESIGN AND MANUFACTURING OF THE WIND TUNNEL TEST MODEL

6.1 Main specifications

To comply with project requirements, the model specifications were defined to allow the investigation of the gust effects on the aerodynamic and aeroelastic model behaviour and the achievement of real time demonstration of active gust load alleviation functions.

The WTT model is composed of a 3D swept wing and a fuselage, built on an ONERA geometry, already used in the past in other WT test campaigns to investigate transonic phenomena and to develop numerical tools [13]. A general model arrangement is illustrated in Figure 26, depicting the half model to be placed inside the WT, together with primary and secondary shafts, flexible coupling, bearings, supporting structures. A suitable control surface (aileron) is integrated in the wing model, located close to the wing tip, and remotely actuated by means of a suitable high-frequency actuation system. A short description of the designed model parts is provided in the following sections, summarizing the design and sizing tasks, the manufacturing and assembling activities performed with the GUDGET Consortium.

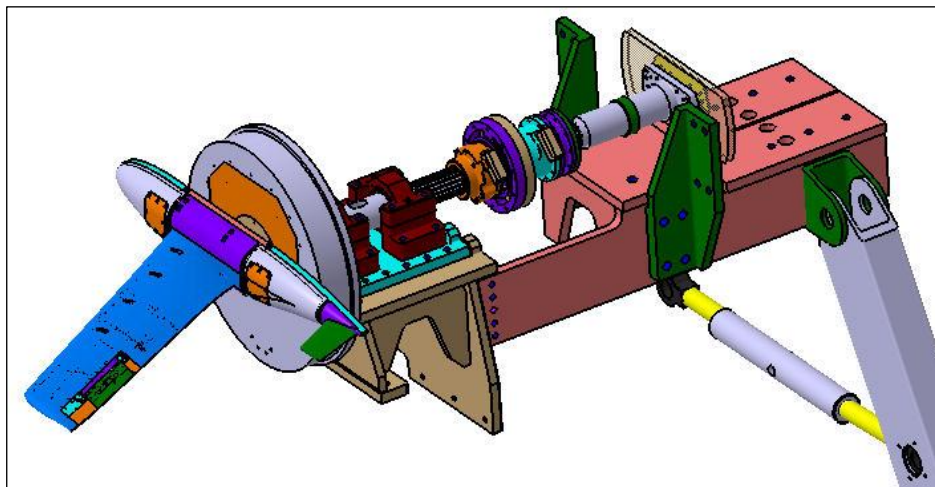


Figure 26 : General arrangement of the WTT model parts

6.2 Main Wing Part

The main wing part (span = 0.6 m) is created from one main body (high performances steel). The wing panel has several pockets for instrumentation channels and cable routing as well as a large aileron actuation pocket, all pockets and covers are located on the lower side of the wing (pressure side). In the outboard region, a subassembly housing actuators, kinematics, aileron, and related instrumentation is attached. An overview of the full wing assembly is shown in Figure 27.

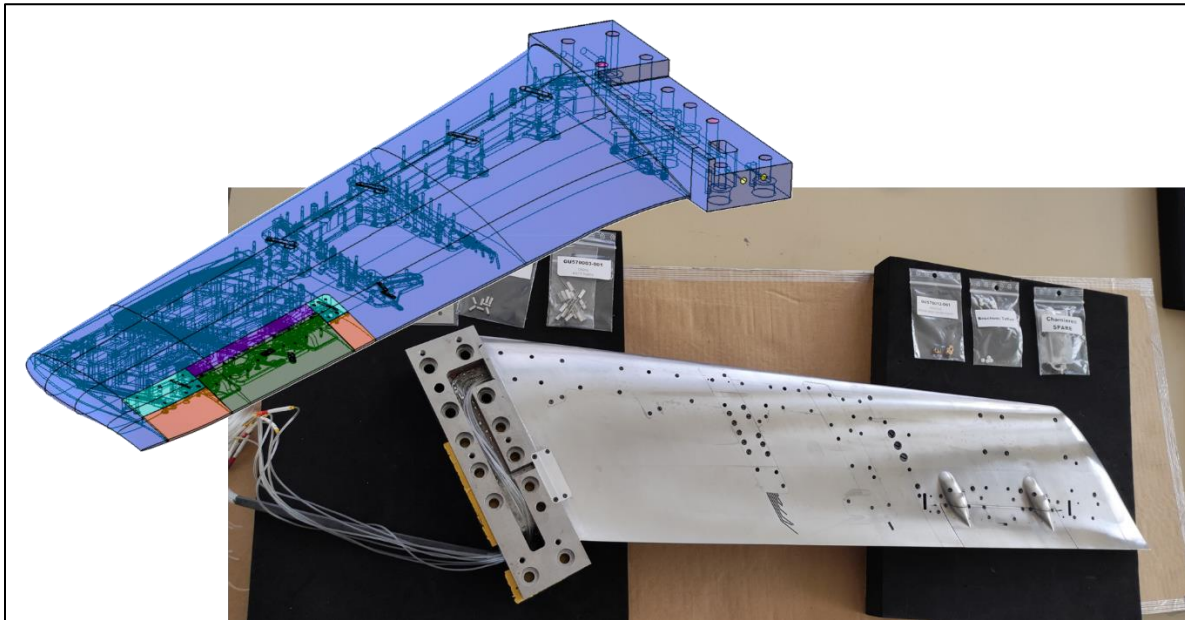


Figure 27 : Wing assembly, CAD view (left) and Manufactured model (right)

A main instrumentation channel is used to route all cables and tubes through the body up to the attachment area. The wing is equipped with a section of 29 static pressure sensors made by pressure tapping. Unsteady pressure measurements are installed in two different sections: an inner section with 17 measurement positions and an outer section containing 14 measurement positions. Four sections on the wing are equipped with strain gauges and 8 accelerometers are placed in three sections.

The main wing panel is attached to a model primary shaft, whose hollow core is also used for all cable and tube routing and attachment of the main fuselage frame.

6.3 Dynamic external aileron

In order to perform a demonstration of active gust alleviation during wing tunnel tests, the model is equipped with an external aileron dynamically actuated and remotely controlled. The dimensions of the aileron are a 25% wing chord (hinge axis located at 75% of the wing airfoil) and a span between 65 and 85% of the wing span. Regarding the small dimensions of the wing, the design of an innovative actuating device has been a challenging topic and the actuation requirements have been limited to deflections in the range of $[-1^\circ, +1^\circ]$ while ensuring dynamic for frequency bandwidth of $[0 - 100]$ Hz.

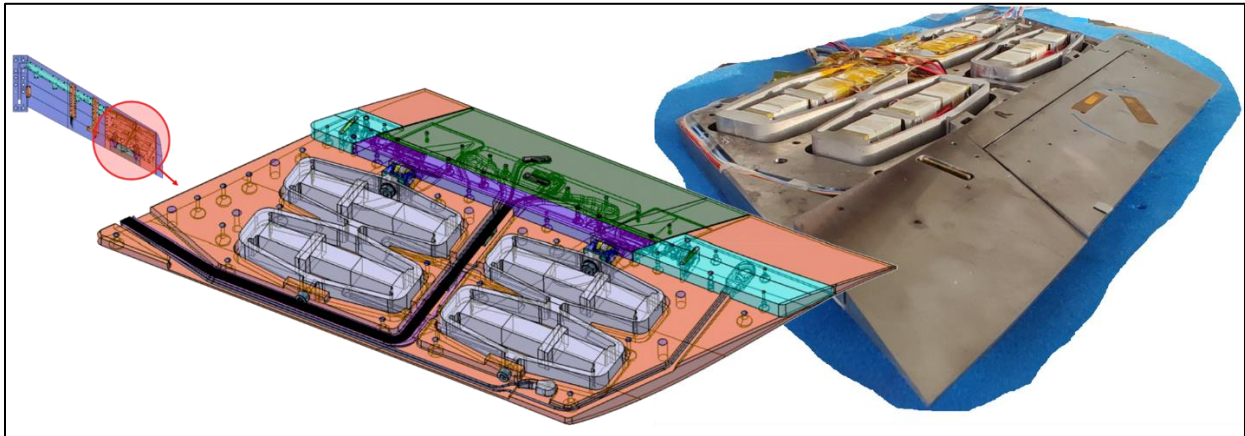


Figure 28 : Outboard wing and external aileron (CAD view– Manufactured Parts)

The aileron actuation is illustrated in Figure 28. Its principle is based on piezoelectric actuators, which linear movement is converted into the aileron rotation by means of a specific high-precision bell-crank link mechanism. The lever arm between the aileron and the actuator allows to specify the needed force and displacement for the actuator (i.e. hinge moment and stroke of the aileron). The final design solution is composed of two actuators installed into specific pockets, to work in parallel in a synchronized manner. Each actuator consists of two piezoelectric actuators in series, as reported in [11]. Since the aileron linkage protrudes the wing aerodynamic shape in the aileron region, two specific fairings were designed to house them.

6.4 Wind tunnel model supporting structure

At the beginning of the project, specifications have been established to define several boundary conditions of the model to allow the investigation of several configurations:

- A rigid configuration: the model attachment is completely rigid and allows only the setting of the angle of attack (steady value),
- A flexible configuration: the model attachment includes a flexibility in pitch motion, along the span axis. This configuration is characterized by a pitch degree of freedom (dynamic vibration mode) allowing the study of free response of this “rigid-body” mode,
- A forced motion configuration: a dynamic actuating device allows to move dynamically the model in pitch (with adjustable frequency and amplitude parameters), along the span axis.

The WT model, interfaces and especially supporting structures have been designed in order to meet these requirements and are depicted in Figure 29, with the indication of all the main components.

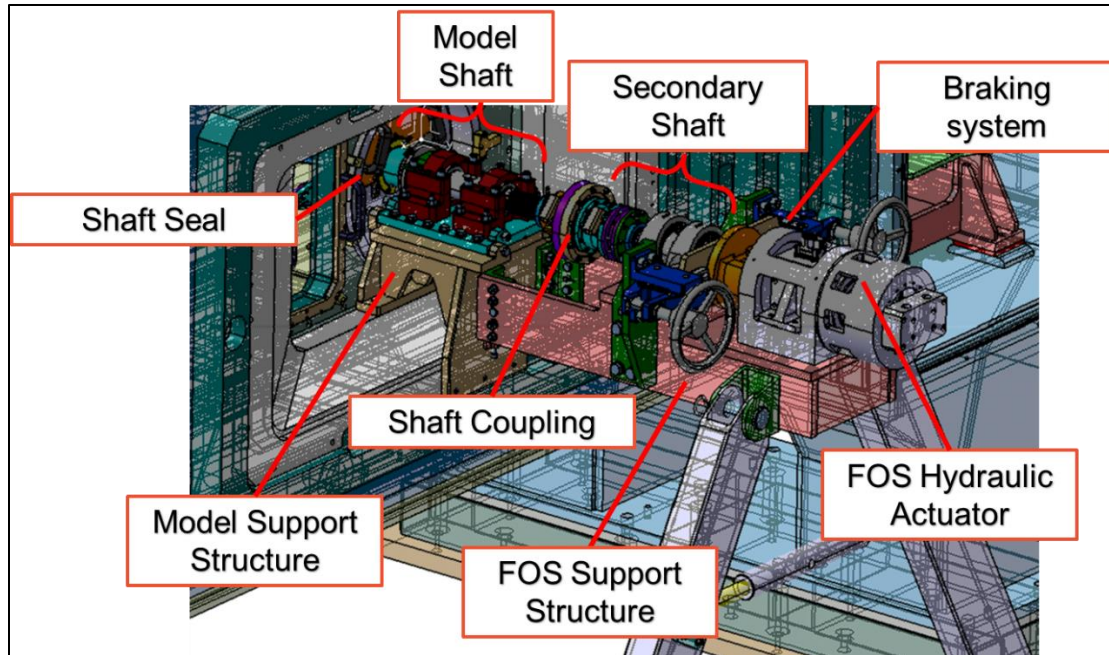


Figure 29 : WT model supporting structure assembly with all the main components

The main model shaft is placed on a suitable model support structure, where a bearings plate is mounted on. The shaft coupling is designed to provide rigid or flexible connection and to permit very fast changes of configurations. Configuration changes between rigid and flexible couplings are made by sliding axially the coupling over main and secondary shafts. The flexible coupling element is a spiral arm torsional spring which stiffness was tuned to adjust the natural frequency of a pitch rigid body mode. The secondary shaft is supported by two ball bearings and connected to a braking system and a forced oscillation system. The latter device was composed of servo-hydraulic actuator and allowed to set the angle of attack of the model.

7 CONCLUSIONS

Within the Clean Sky 2 AIRFRAME ITD framework, this paper presents a research program conducted in the NACOR project and centred on Wind Tunnel Tests conducted at the transonic ONERA S3Ch facility. The program's objective is to deepen our understanding of gust effects and evaluate advanced load control methods.

The initial phase, under the GIDGET project, focused on developing an innovative test rig for investigating transonic gust loads within the aim to generate gusts with higher amplitudes than previous tests, specifically to analyse non-linear phenomena induced by gusts. Design activities and parametric analyses resulted in the development of new devices capable of generating harmonic and cylindrical gusts across wide amplitude and frequency ranges. Two concepts, involving a configuration of 2 airfoils positioned upstream of the test section, were explored: the first one with dynamically movable flapped airfoils and the second based on fixed vanes with active flow control. While both concepts showed interesting innovative and functional aspects,

their performances were limited during the first ONERA WTT campaign. The study of complex phenomena, especially in highly loaded and transonic flows, presents challenges in system design. Nonetheless, both gust generation concepts hold significant promise for applications and wind tunnel tests, and could be revisited and optimized in future research programs.

The test rig also included a wall-mounted half-wing model equipped with a remote-controlled dynamic aileron. The main outcomes and insights of a second WTT campaign (illustrated in Figure 30) , focused on analysing gust effects on this model under varying aerodynamic or structural conditions, are discussed in a companion paper [12].

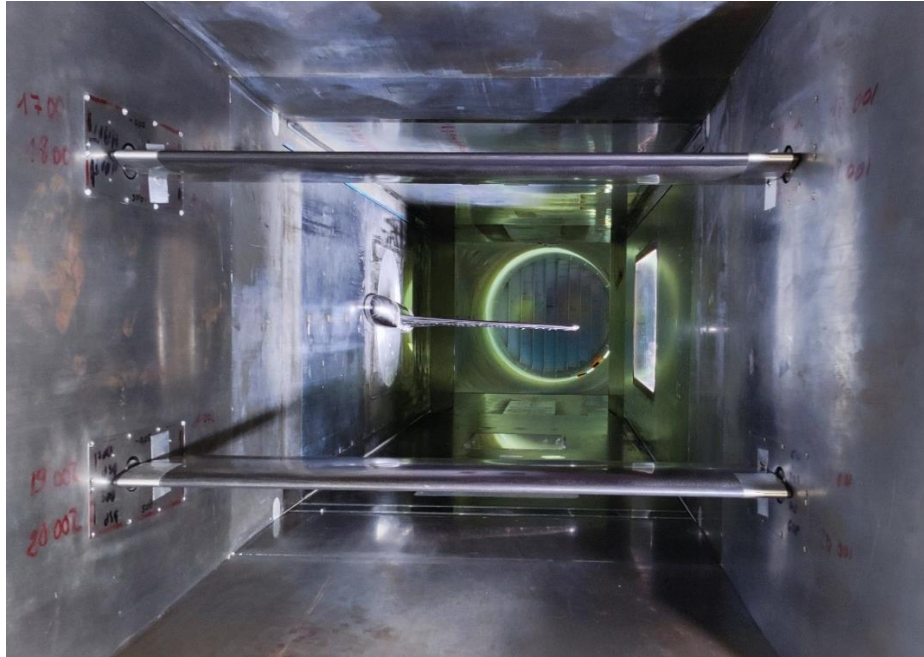


Figure 30 : Arrangement of the experimental set-up: the gust generator (foreground) and the half wing model (background)

REFERENCES

- [1] Strategic Research & Innovation Agenda (SRIA) 2017 update, executive summary, Advisory Council for Aviation Research and Innovation in Europe, ACARE.
- [2] <https://www.clean-aviation.eu/clean-sky-2>
- [3] Lancelot PMGJ et al., Design and testing of a low subsonic wind tunnel gust generator, *Advances in Aircraft and Spacecraft Science*, Vol. 4, No. 2 (2017) 125-144
- [4] Lepage A. et al., A complete experimental investigation of gust load: from generation to active control, *IFASD*, 2015, Saint Petersburg
- [5] Tang D.M. et al., Experiments and Analysis for a gust generator in a wind tunnel, *Journal of Aircraft*, Vol. 33, N°1, Jan-Fev 1996.

- [6] Brion, V. et al., Generation of vertical gusts in a transonic wind tunnel, *Experiments in Fluids*, 2015, 56(7), 1-16.
- [7] Allen, N.J. and Quinn, M., Development of a Transonic Gust Rig for Simulation of Vertical Gusts on Half-models, *31st AIAA Aerodynamic Measurement Technology and Ground Testing Conference*, 2015, Dallas.
- [8] Dandois J. et al., Open and closed-loop control of transonic buffet on 3D turbulent wings using fluidic devices, *Comptes Rendus de Mécanique*, June 2014, Volume 342, Issue 6-7.
- [9] Natale N., Russo S., Dequand S., Lepage A., Paletta N., Aerodynamic Design of Airfoil Shape for Gust Generation in a Transonic Wind Tunnel, *Aerotecnica Missili & Spazio*, 2021, 100:345–362
- [10] <https://cedrat-technologies.com/wp-content/uploads/2023/03/VIPER.pdf>
- [11] https://cedrat-technologies.com/wp-content/uploads/2023/03/GUDGET_PROJECT.pdf
- [12] Vincent Bouillaut et al., Wind Tunnel Tests for Gust Load Investigation in transonic flows – Part 2 : Experimental results and control demonstration, *IFASD*, 2024, *Den Haag*
- [13] P. Molton et al. “Control of Buffet Phenomenon on a Transonic Swept Wing”, *AIAA JOURNAL*, Vol. 51, No. 4, April 2013

ACKNOWLEDGEMENTS

The ONERA works have been funded within the frame of the Joint Technology Initiative JTI Clean Sky 2, AIRFRAME Integrated Technology Demonstrator platform "AIRFRAME ITD" (NACOR project - contract N. CS2-AIR-GAM-2020-21-04) being part of the Horizon 2020 research and Innovation framework program of the European Commission.

The GUDGET project has received funding from the Clean Sky 2 Joint Undertaking under the European Union’s Horizon 2020 research and innovation programme under grant agreement No 831802.



COPYRIGHT STATEMENT

The authors confirm that they, and/or their company or organisation, hold copyright on all of the original material included in this paper. The authors also confirm that they have obtained permission from the copyright holder of any third-party material included in this paper to publish it as part of their paper. The authors confirm that they give permission, or have obtained permission from the copyright holder of this paper, for the publication and public distribution of this paper as part of the IFASD 2024 proceedings or as individual off-prints from the proceedings.